

Data-Driven Identification of Governing Partial Differential Equations for the Transmission Line Systems

Yanming Zhang and Lijun Jiang*

Abstract—Discovering governing equations for transmission line is essential for the study on its properties, especially when the nonlinearity is introduced in a transmission line system. In this paper, we propose a novel data-driven approach for deriving the governing partial differential equations based on the spatial-temporal samples of current and voltage in the transmission line system. The proposed method is based on the ridge regression algorithm to determine the active spatial differential terms from the candidate library that includes nonlinear functions, in which the time and spatial derivatives are estimated by using polynomial interpolation. Three examples, including uniform and nonuniform transmission lines and a specific type of nonlinear transmission line for soliton generation, are provided to benchmark the performance of the proposed approach. The results demonstrate that the newly proposed approach can inverse the distributed circuit parameters and also discover the governing partial differential equations in the linear and nonlinear transmission line systems. Our proposed data-driven method for deriving governing equations could provide a practical tool in transmission line modeling.

1. INTRODUCTION

It is well known that transmission line systems, as the signal carrier, have been widely used in microwave circuits [1–7]. It is often assumed that homogeneous conductors are parallel to ground, and thereby the line parameters are uniform [1, 2]. There are, however, some cases of sophisticated structures such as nonuniform transmission lines with strong longitudinal variation in the line parameters [3–6] and nonlinear transmission lines with nonlinear elements that may be nonlinear magnetic materials, nonlinear dielectric materials, or both [7]. This nonuniformity and nonlinearity bring nonlinear terms in the governing equations and make the system characterization and modeling very difficult.

Recently, data-driven discovery approaches, considered as the fourth science paradigm after empirical, theoretical, and computational technology [8], have been widely expanded and utilized in engineering and physical science [9]. They discover models of the evolution law, i.e., the governing equations in a dynamic system, merely via the simulated or measured data. Thereinto, several methods have been proposed, such as empirical dynamic modeling [10, 11], equation-free modeling [12], nonlinear regression [13–15], artificial neural networks [16], nonlinear Laplacian spectral analysis [17], modeling emergent behavior [18], normal form identification [19], and automated inference of dynamics [20]. To sum up, we have classified seminal contributions into three types as

- 1) The symbolic regression is first proposed to determine the governing equations from data directly. The steps are to calculate the numerical differentiation of experimental data first and then apply symbolic regression based on the evolutionary algorithm to compare with analytical derivative solutions. Eventually, the nonlinear dynamic system is determined [21, 22].

Received 27 October 2020, Accepted 21 December 2020, Scheduled 31 December 2020

* Corresponding author: Lijun Jiang (jianglj@hku.hk).

The authors are with the Department of Electrical and Electronic Engineering, the University of Hong Kong, Pokfulam, Hong Kong, China.

- 2) The neural network-based framework is explored to learn unknown parameters in the partial differential equation, in which the form of the nonlinear response function in the equations has been determined [23–25]. However, these specific forms of the governing equation are usually unknown in advance. Consequently, identification governing equations with a less restrictive setting remains a great challenge.
- 3) More recently, sparse identification of nonlinear dynamics (SIND) is developed based on the combination of the sparsity and symbolic regression [26–29]. The key idea is to build a library of hypothetical functions that have the possibility to appear in the actual equations. Afterward, by taking the advantages of sparsity promoting regression techniques, the active candidate terms are selected, and thereby the governing equations are determined.

These recent studies have significantly advanced the progress of the partial differential equation identification from the observed data. However, there are still some issues among these methods. To be specific, the symbolic regression is so highly computationally expensive that it is challenging to apply this method in dealing with large-scale data due to the unacceptable computation cost. Neural network-based approach requires appropriate prior knowledge on the mechanisms of the dynamics, which is usually hard to acquire in advance. Thanks to the sparse promoting regression in SIND, it has been proved to robustly determine, in a highly efficient computational manner, the governing equations in hydrodynamics [28], chaotic system [29], biological network [30], and material science [31]. Hence, taking advantage of SIND, we could utilize this data-driven approach for the analysis and modeling of complex transmission line system, especially for the identification of governing equations when only the transient measured or simulated data are available.

In this paper, we propose a ridge regression-based SIND approach to identify a set of partial differential equations of the current and voltage in the transmission line systems. Based on the spatial-temporal samples of current and voltage, the hypothetical spatial differential functions are calculated to build the candidate library. Then, the ridge regression is applied to select the active terms in the library. Finally, the governing equations of the transmission line are extracted. Three cases, including the uniform transmission line, nonuniform transmission line, and a type of nonlinear transmission line for the solitons generation, are investigated to verify the proposed method. And the accuracy of our novel approach is acceptable to engineering applications. The proposed data-driven approach will pay the way for deriving governing equations for complex transmission line systems.

The organization of this paper is as follows. The proposed method for deriving the governing partial differential equations from the observation is introduced in Section 2. Then three examples, namely uniform transmission line, nonuniform transmission line, and nonlinear transmission line, are provided to demonstrate the effectiveness and robustness of the proposed method in Section 3. Finally, the conclusions are summarized in Section 4.

2. METHODS

Without losing the generality, we assume transmission line variables including voltage $u(z, t)$ and current $i(z, t)$ in a one-dimensional space z varying with time t . The general form of their governing equations can be written as

$$u_t = f_1(z, u, i, u_z, i_z, u_{zz}, i_{zz}, uu_z, ii_z, \dots) \quad (1)$$

$$i_t = f_2(z, u, i, u_z, i_z, u_{zz}, i_{zz}, uu_z, ii_z, \dots) \quad (2)$$

where subscripts denote partial differentiation in the either spatial or temporal domain; $f_1(\cdot)$ and $f_2(\cdot)$ refer to the unknown function of all possible terms that could appear in the governing equation of voltage and current in the transmission line system. Based on this assumption, we want to determine actual terms and thereby discover the governing equations of the transmission line system from a series of measurements of voltage $u(z, t)$ and current $i(z, t)$.

2.1. Data-Driven Scheme for the Identification of Governing Equation

As shown in Eqs. (1) and (2), $f_1(\cdot)$ and $f_2(\cdot)$ include the large collection of candidate terms for constructing the governing equation of the transmission line system, which can be considered as a

library. Based on the spatiotemporal data from the observation, we can construct each candidate term by taking the derivatives of the data with respect to the spatial dimension so that the right-hand side of Eqs. (1) and (2) is built. Similarly, the left-hand side of Eqs. (1) and (2)) can be obtained by taking the derivatives of the data with time. In the following, we will first demonstrate the identification of the governing equation of u_t in Eq. (1).

To be specific, we denote \mathbf{U} and \mathbf{I} to be matrices containing the values of $u(z, t)$ and $i(z, t)$, respectively. After taking the derivatives of the data with respect to the spatial dimension, the library of candidate terms that may appear in $f_1(\cdot)$ are combined into a matrix $\Theta(\mathbf{U}, \mathbf{I})$:

$$\Theta(\mathbf{U}, \mathbf{I}) = [\mathbf{Z} \ \mathbf{U} \ \mathbf{I} \ \mathbf{U}_z \ \mathbf{I}_z \ \mathbf{U}_{zz} \ \mathbf{I}_{zz} \ \mathbf{U}\mathbf{U}_z \ \mathbf{I}\mathbf{I}_z \ \dots] \tag{3}$$

Each column of Θ contains all of the values of a particular candidate function across all of the grid points from the collected data. In particular, suppose that we obtain $u(z, t)$ and $i(z, t)$ on an $n \times m$ grid, which means that there are n spatial observations at m time points. There are l candidate terms in the $f_1(\cdot)$, then $\Theta \in \mathbb{C}^{m \cdot n \times l}$. We also take the derivative with respect to time to obtain \mathbf{U}_t and reshape it into a column vector just like we did the columns of Θ , where $\mathbf{U}_t \in \mathbb{C}^{m \cdot n \times 1}$. Hence, from the observed data and the corresponding derivatives, we can utilize a linear equation to represent the general form of partial differential equation as shown in Eq. (1):

$$\mathbf{U}_t = \Theta(\mathbf{U}, \mathbf{I})\beta \tag{4}$$

where β is a vector of coefficients of each candidate term, and we define β as $\beta = [\beta_1, \beta_2, \beta_3, \dots, \beta_l]^T$. Then the linear equation of Eq. (4) can be expressed in the form of elements, as shown in Eq. (5).

$$\begin{bmatrix} u_t(z_0, t_0) \\ u_t(z_1, t_0) \\ u_t(z_2, t_0) \\ \vdots \\ u_t(z_{n-1}, t_m) \\ u_t(z_n, t_m) \end{bmatrix} = \underbrace{\begin{bmatrix} 1 & u(z_0, t_0) & i(z_0, t_0) & \dots & ii_z(z_0, t_0) & \dots \\ 1 & u(z_1, t_0) & i(z_1, t_0) & \dots & ii_z(z_1, t_0) & \dots \\ 1 & u(z_2, t_0) & i(z_2, t_0) & \dots & ii_z(z_2, t_0) & \dots \\ \vdots & \vdots & \vdots & \vdots & \ddots & \vdots \\ 1 & u(z_{n-1}, t_m) & i(z_{n-1}, t_m) & \dots & ii_z(z_{n-1}, t_m) & \dots \\ 1 & u(z_n, t_m) & i(z_n, t_m) & \dots & ii_z(z_n, t_m) & \dots \end{bmatrix}}_{\text{Example } \Theta \text{ for the hypothetical partial differentiation in the spatial domain}} \begin{bmatrix} \beta_1 \\ \beta_2 \\ \vdots \\ \beta_l \end{bmatrix} \tag{5}$$

Example Θ for the hypothetical partial differentiation in the spatial domain

It is worth noting that when we consider nonlinear characteristics in the transmission line system, the library Θ should be assumed to have a sufficiently abundant column space to ensure that these nonlinear dynamics of the transmission line are included in the assumed library. Then the actual partial differential equations can be well-expressed by Eq. (4) with a sparse vector of coefficients β . That is to say, enough candidate functions should be constructed for the selection so that the governing partial differential equation can be represented as a weighted sum. Each row of this linear equation represents an observation of dynamic characteristics of the current and voltage at a particular point in time and space, which can be written as

$$u_t(z, t) = \sum_j \Theta_j(u(z, t), i(z, t))\beta_j \tag{6}$$

where the coefficient β_j corresponds to weights for the j th candidate term. The non-zero weight means that the corresponding candidate term appears in the actual governing partial differential equation.

Figure 1 shows the architecture of the data-driven method of discovery partial differential equation of u_t in the transmission lines. The steps are listed as follows.

- 1) Collect data of voltage $u(z, t)$ and current $i(z, t)$ from the observation.
- 2) Determine the derivative with respect to time and spatial domain according to the candidate terms in the library.
- 3) Construct the line equation based on matrix \mathbf{U}_t and $\Theta(\mathbf{U}, \mathbf{I})$.
- 4) Obtain the coefficient vector β by solving the regression.
- 5) Identify the partial differential equations according to the non-zero coefficient in β .

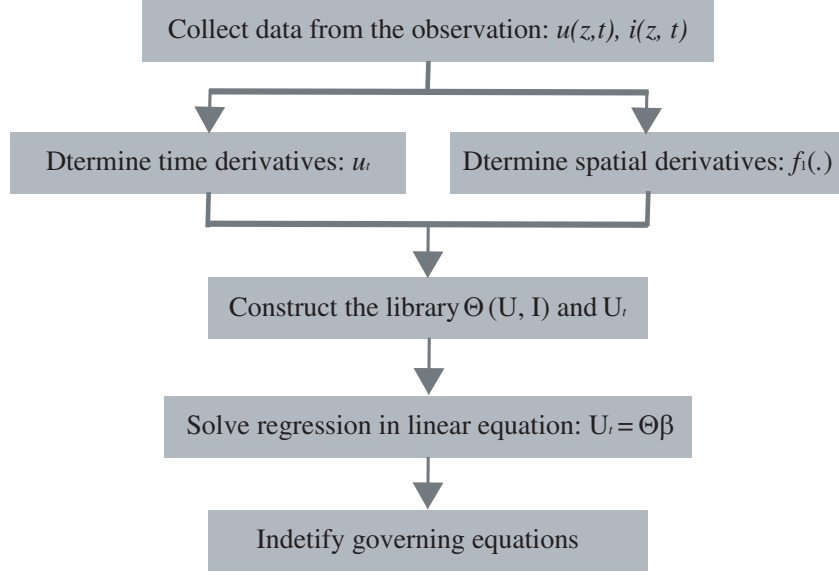


Figure 1. The architecture of discovering the partial differential equation of the voltage and current in the transmission line system.

2.2. The Regression Framework

To discover the coefficients β , we could utilize the least-squares method for an unbiased representation of the dynamics, where the loss function is defined as

$$L_{LSM} = \|\Theta\beta - \mathbf{U}_t\|_2^2 \quad (7)$$

And the unbiased solution of this least-squares problem is given as follows

$$\begin{aligned} \hat{\beta}^{LSM} &= \operatorname{argmin}_{\beta} \|\Theta\beta - \mathbf{U}_t\|_2^2 \\ &= (\Theta^T \Theta)^{-1} \Theta^T \mathbf{U}_t \end{aligned} \quad (8)$$

The least-squares method does offer the solution with the lowest residual sum of squares (RSS), but not the best solution in most cases because it could easily lead to overfitting issues, especially for noisy data. Another significant shortcoming is that, due to correlations in Θ , the least-squares problem is poorly conditioned. Specifically, error in computing the derivatives (already an ill-conditioned issue in the least-squares method) will be magnified by numerical errors when inverting Θ . Thus if least squares method is utilized, it can radically change the qualitative nature of the inferred dynamics in the transmission line systems. Instead, we use ridge regression that can be considered as a linear regression with the penalty to avoid the overfitting issues and ill-conditioned problems [32], where the corresponding loss function is expressed as

$$L_{ridge} = \|\Theta\beta - \mathbf{U}_t\|_2^2 + k\|\beta\|_2^2 \quad (9)$$

where k refers to the regularization parameter. It is worth noting that the first term in Eq. (9) is basically loss function in the least-squares method, and then the second term with β is what makes penalty in ridge regression. This regularization assures that active terms will only show up in the identified partial differential equation if their effect on the error $\|\Theta\hat{\beta} - \mathbf{U}_t\|$ outweighs their addition to $\|\hat{\beta}\|$, which avoid the overfitting issues. The general solution of the ridge regression is given as follows [33]

$$\begin{aligned} \hat{\beta}^{ridge} &= \operatorname{argmin}_{\beta} \|\Theta\beta - \mathbf{U}_t\|_2^2 + k\|\beta\|_2^2 \\ &= (\Theta^T \Theta + kI)^{-1} \Theta^T \mathbf{U}_t \end{aligned} \quad (10)$$

Comparing with Eqs. (8) and (10), we can see that the condition number of matrix $(\Theta^T \Theta + kI)^{-1}$ is better than that of matrix $(\Theta^T \Theta)^{-1}$ when there is high correlations in Θ .

We use sequential threshold ridge regression (STRR) algorithm to obtain the solution of Eq. (10) [28]. Inspired by using sequential threshold least squares (STLS) to solve least squares, we determine the coefficient β by artificially setting a hard threshold tolerance tol in the ridge regression. As shown in Algorithm 1, if the coefficient β_j is less than tol , then it is forced to set to 0, and the corresponding candidate terms are discarded in the next regression. Finally, the active terms are determined only if the corresponding β_j are always greater than tol in the iterative regressions.

Algorithm 1 The sequential threshold ridge regression: STRR($\Theta, \mathbf{U}_t, k, tol, iter$)

Require:

The constructed library: Θ ; Time derivative matrix: \mathbf{U}_t ; Regularization parameter: k ; Threshold tolerance: tol ; Iterations: $iter$;

Ensure:

The ridge regression predictor: $\hat{\beta}$;

1: Ridge regression: $\hat{\beta} = \operatorname{argmin}_{\beta} \|\Theta\beta - \mathbf{U}_t\|_2^2 + k\|\beta\|_2^2$

2: Select large coefficients: $\text{bigcoeffs} = \{j : |\beta_j| \geq tol\}$

3: Apply hard threshold: $\hat{\beta}[\sim \text{bigcoeffs}] = 0$

4: Recursive call with fewer coefficients: $\hat{\beta}[\text{bigcoeffs}] = \text{STRR}(\Theta[:, \text{bigcoeffs}], \mathbf{U}_t, k, tol, \text{iters} - 1)$

5: **return** $\hat{\beta}$;

2.3. Numerical Differentiation

In the discovery of partial differential equation processing, we need to take the derivatives of the data of current and voltage with respect to time and spatial dimension to construct the matrix \mathbf{U}_t and Θ , respectively. For the clean (noise-free) data, the finite difference methods can be utilized to achieve \mathbf{U}_t and Θ [34–36]. Here, we take the first-order time derivative of $u(t, \cdot)$ as an example, and the backward difference formula is defined as follows

$$u_t(t_i, \cdot) = \frac{u(t_i, \cdot) - u(t_{i-1}, \cdot)}{\Delta t} + O(\Delta t) \quad (11)$$

The forward difference formula is defined as

$$u_t(t_i, \cdot) = \frac{u(t_{i+1}, \cdot) - u(t_i, \cdot)}{\Delta t} + O(\Delta t) \quad (12)$$

And the central difference formula with second-order accurate is expressed as

$$u_t(t_i, \cdot) = \frac{u(t_{i+1}, \cdot) - u(t_{i-1}, \cdot)}{2\Delta t} + O((\Delta t)^2) \quad (13)$$

Similarly, the spatial derivatives can also be obtained by the finite difference methods to construct the matrix Θ [34] for the clean data. However, it is still challenging to achieve accurate numerical derivatives of noisy data because the noise brings the error in the derivative terms. To alleviate the noise interference in the calculation of derivatives, several methods are proposed, such as smoothing technique, Tikhonov differentiation, and spectral differentiation based on the discrete Fourier transform for the periodic signals. Thereinto, it is found that the polynomial interpolation can effectively and robustly calculate the derivatives of noisy data [37, 38]. The main idea is that, for each grid where we calculate the derivative, a polynomial with the degree of p is fit to greater than p grids. Then, we compute the derivatives of the obtained polynomial to approximate those of the collected voltage or current data. It is worth noting that it is difficult to fit a polynomial for the grids which are close to the boundary. Thus, current or voltage in these grids is discarded in the regression.

2.4. Subsampling Data

When the large datasets of current and voltage are collected in the transmission line system, the subsampling processing can be applied to improve regression efficiency. Specifically, we randomly pick a

fraction of the whole data through choosing a set of spatial grids and evenly sampling the data in time with a higher sampling interval than that in the original dataset. That is to say, a part of the rows in the linear equation $\mathbf{U}_t = \Theta(\mathbf{U}, \mathbf{I})\beta$ are discarded. It is worth noting that while only these subsampled data of current and voltage are employed in the regression of linear equation, the derivatives are calculated through polynomial interpolation, which still needs the information of several adjacent grid points to fit the polynomial.

3. RESULTS

In this section, we analyze three cases of transmission line systems, namely the uniform transmission line, nonuniform transmission line, and a specific nonlinear transmission line for the soliton generation, to validate the proposed method. The numerical simulation based on the FDTD method or the analytic solutions of the governing equations is applied to provide the spatial-temporal data of the current and voltage in these cases.

3.1. Uniform Transmission Line

We first consider a uniform transmission line to demonstrate our proposed method, as shown in Fig. 2(a). A driven voltage source, $v(t)$, with an internal resistance, $R1 = 100 \Omega$, is loaded at port 1. Port 2 is loaded with 200Ω resistors and then shorted to the reference conductor. The distributed parameter circuit of the uniform transmission line is plotted in Fig. 2(b), where R, L, G, C are the per-unit-length (p.u.l.) series resistance, series inductance, shunt conductance, and shunt capacitance, respectively. It is well known that the telegrapher's equations are the governing equations in such a system, and they can be expressed as

$$\begin{aligned} \frac{\partial i(z, t)}{\partial t} &= -\frac{1}{L} \frac{\partial u(z, t)}{\partial z} - \frac{R}{L} i(z, t) \\ \frac{\partial u(z, t)}{\partial t} &= -\frac{1}{C} \frac{\partial i(z, t)}{\partial z} - \frac{G}{C} u(z, t) \end{aligned} \quad (14)$$

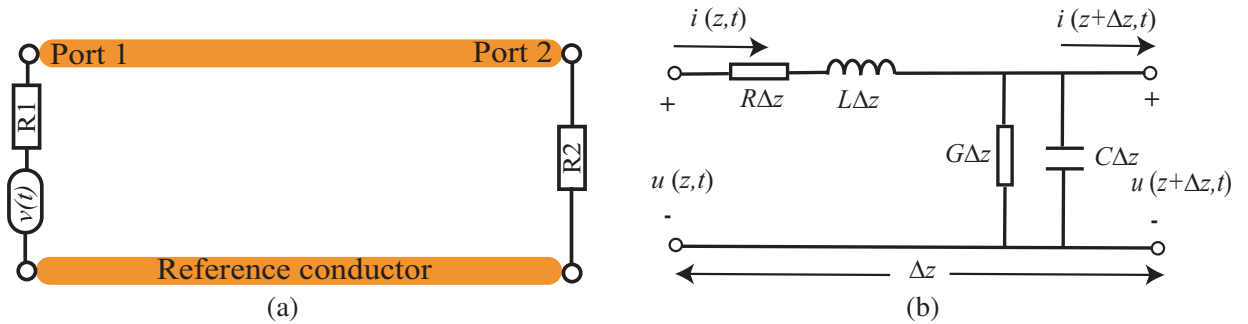


Figure 2. (a) The design scheme of uniform transmission line. (b) The distributed parameter circuit of the uniform transmission.

We define that the circuit is excited by double exponential waveform voltage source, $v(t) = 60 \times (\exp(-8 \times 10^5 t) - \exp(-1 \times 10^6 t))$ V, and the line parameters are $R = 0$, $G = 0$, $L = 2.5 \times 10^{-7}$ H/m, $C = 1 \times 10^{-10}$ F/m. The FDTD method is applied to simulate the solution of the current and voltage. To implement FDTD, it is assumed that the line is divided into M segments with equal length Δz . We interlace the $M + 1$ voltage points (u_1, u_2, \dots, u_{M+1}) and M current points (i_1, i_2, \dots, i_M), and the current points at two ends are i_0 and i_{M+1} . Each voltage and adjacent current solution point are separated by $\Delta z/2$, as shown in Fig. 3. Then, the spatial derivatives of voltage and current points are approximated by central differences. At the two end points, forward and backward difference schemes are used. The implementation of FDTD is provided in Appendix A in detail. Courant-Friedrichs-Levy (CFL) condition is adopted to ensure the stability in FDTD simulation.

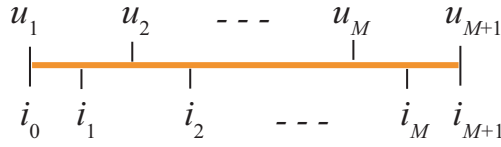


Figure 3. Discretization of the voltages and currents along the line.

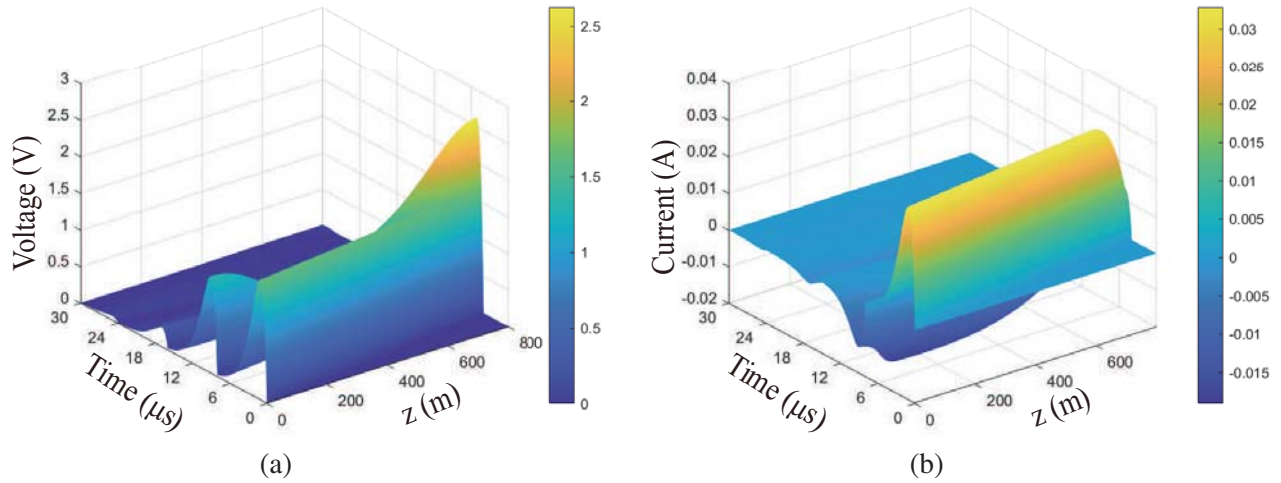


Figure 4. (a) The simulated voltage distribution. (b) The simulated current distribution.

Figure 4 shows the simulated spatial-temporal distribution of the voltage and current along the line, respectively. We randomly select 100 spatial grids and 60 time grids between 6 μs and 7 μs from the simulated data to build the line equations of the voltage: $\mathbf{U}_t = \Theta_1 \beta_1$ and current: $\mathbf{I}_t = \Theta_2 \beta_2$ (see Eqs. (4) and (5)). The library including candidate terms are assumed as follows

$$\Theta_1 = \Theta_2 = [\mathbf{Z} \ \mathbf{U} \ \mathbf{I} \ \mathbf{U}_z \ \mathbf{I}_z \ \mathbf{U}_{zz} \ \mathbf{I}_{zz}] \tag{15}$$

Then, based on the subsampled spatial-temporal data, the corresponding derivatives including matrix \mathbf{U}_t , \mathbf{I}_t , Θ_1 , and Θ_2 are determined after fitting to the Chebyshev polynomial with the degree of 4. It is worth noting that, as long as the polynomial interpolation can achieve the accurate fitting, other kinds of polynomial function can also be adopted here. Through the ridge regression, the coefficient of \mathbf{I}_z is extracted with a value of -1.004×10^{10} in β_1 , and the coefficient of \mathbf{U}_z is extracted with a value of 4.07×10^6 in β_2 . Consequently, the partial differential equations are identified as: $u_t = -1.004 \times 10^{10} i_z$, $i_t = 4.07 \times 10^6 u_z$. Clearly, the derived partial differential equation consists of the actual governing equation in the transmission line system. Besides, the comparison between the actual and extracted distributed parameters is also shown in Table 1. It can be seen that the line parameters are extracted exactly.

Table 1. The identification results for the uniform transmission line.

Parameter	Actual value	Extracted value	Error
L	2.5×10^{-7}	2.45×10^{-7}	2%
C	1×10^{-10}	9.96×10^{-11}	0.4%

3.2. Nonuniform Transmission Line

The second case is an ideal lossless nonuniform transmission line, in which the line parameter is modeled by an ideal linear relationship along with the line position [6, 39, 40]. A normal expression of the

distributed parameter that is dependent on the position along the line can be written as

$$C(z) \sim \frac{1}{A + Bz} \quad (16)$$

where A , B are constant and slope, respectively. Then, the generalized dynamic voltage equation describing this system can be expressed as

$$\frac{\partial u(z, t)}{\partial t} = -(A + Bz) \frac{\partial i(z, t)}{\partial z} \quad (17)$$

In our simulation, the circuit is excited by the sinusoidal waveform voltage source, $v(t) = 60 \times \sin(6\pi \times 10^6 t)$ V. For the line parameters, the distributed capacitance is given by $\frac{1 \times 10^{-10}}{1 + 0.004 \times z}$ F/m, and the inductance has a constant value of 2.5×10^{-7} H/m. We utilize the FDTD method by modifying the corresponding line parameters to simulate the current and voltage in the transmission line. Figs. 5(a) and (b) show the simulated spatial-temporal distribution of the voltage and current along the line, respectively. We choose 200 spatial grids randomly and 50 time grids between $0.6 \mu\text{s}$ and $0.7 \mu\text{s}$ as input data of the proposed method. The library including candidate terms are assumed as

$$\Theta = [\mathbf{Z} \ \mathbf{U} \ \mathbf{I} \ \mathbf{U}_z \ \mathbf{I}_z \ \mathbf{Z}\mathbf{U}_z \ \mathbf{Z}\mathbf{I}_z \ \mathbf{U}\mathbf{U}_z \ \mathbf{I}\mathbf{I}_z] \quad (18)$$

Then, the time derivatives \mathbf{U}_t and spatial derivatives Θ are determined through fitting to the Chebyshev polynomial with the degree of 4 based on the input data.

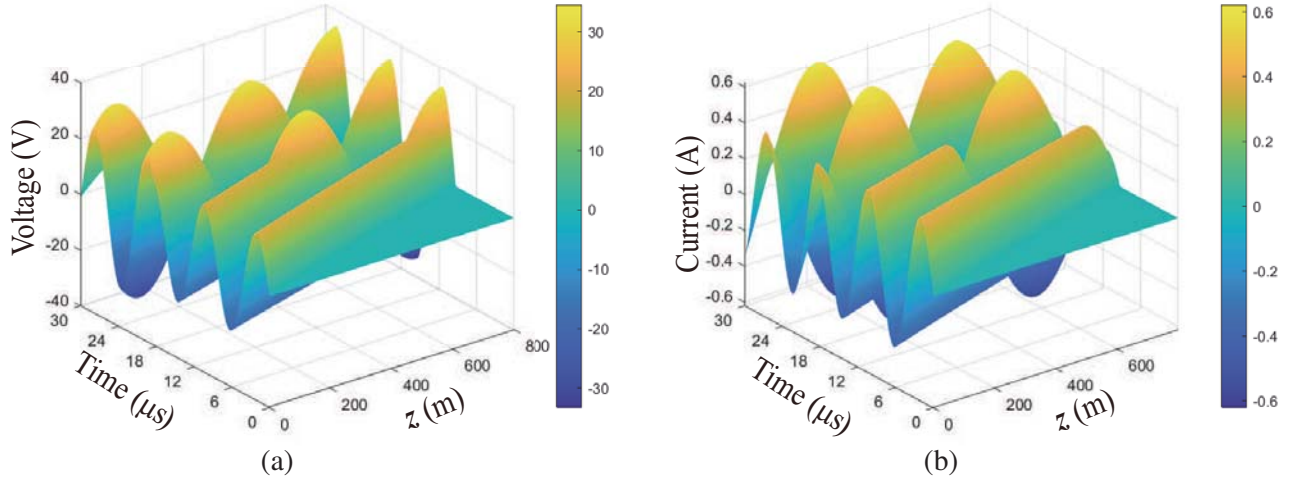


Figure 5. (a) The voltage distribution. (b) The current distribution.

Through the ridge regression, the coefficient of \mathbf{I}_z with a value of -1.09×10^{10} and $\mathbf{Z}\mathbf{I}_z$ with a value of -3.8×10^7 is extracted in β . The comparison between the actual and identified capacitance is shown in Eqs. (19) and (20).

$$\frac{1}{C(z)} \sim 1 \times 10^{-10} + 4 \times 10^7 z \text{ (Actual form)} \quad (19)$$

$$\frac{1}{C(z)} \sim 1.09 \times 10^{-10} + 3.8 \times 10^7 z \text{ (Identified form)} \quad (20)$$

It is clear that the identified partial differential equation is consistent with the actual governing equation in the nonuniform transmission line, where the errors of this parameter inversion mainly come from the FDTD simulation and derivative calculations. Hence, our proposed method can still discover the governing equation of the nonuniform transmission line with the known expression of the line parameters.

3.3. Nonlinear Transmission Line

Nonlinear lumped element transmission line systems have a variety of applications and have attracted much attention in theory [7, 41, 42] and experiments [43–45]. Thereinto, one significant application is the generation of solitons for short pulses, shock waves, and high power radio frequency (RF) pulses. It is well known that the Korteweg de Vries (KdV) as a type of nonlinear dispersive differential equations that support soliton solutions can be modeled by a specific electrical transmission line, as shown in Fig. 6. The capacitor C_{nl} is nonlinear, where its relationship with voltage is given by $C_{nl} = C_0 - C_N V$. The inductor L has a dispersive capacitor in parallel C_s . The governing equation can be derived by the perturbation method [7, 41, 42] and is expressed as follows

$$\frac{\partial u}{\partial t} + \frac{C_N}{C_0} u \frac{\partial u}{\partial z} + \frac{C_s}{2C_0} \frac{\partial^3 u}{\partial z^3} = 0 \tag{21}$$

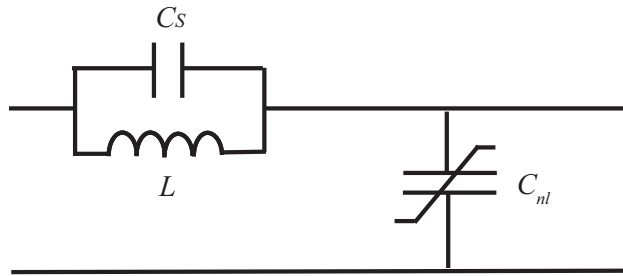


Figure 6. The elementary network with nonlinear and dispersive components.

The analytic solutions to the KdV equation given by inverse spectral transform in [41] are utilized here, and the single soliton solution is represented as

$$u = A_0 \operatorname{sech}^2 \left(\sqrt{\frac{C_N A_0}{6C_s}} \left(z - \frac{C_N A_0}{3C_0} t \right) \right) \tag{22}$$

To validate the proposed method, we merely utilize the observation from the nonlinear transmission line structure shown in Fig. 6 as input data. First, we assume that the parameters in the transmission line are: $\frac{C_N}{C_0} = 6$ and $\frac{C_s}{C_0} = 2$. As shown in Fig. 7(a), two solitons with different amplitudes, namely $A_0^1 = 1$ and $A_0^2 = 2$, then can be observed from the measurement or simulation. Fig. 7(b) shows these two solitons at time $t = 2.5$ s and $t = 5$ s. It is clear that the generated two solitons interact with different velocities during the propagation.

We pick the general form with sufficient spatial differentiation terms to ensure that the nonlinear dynamics induced by the nonlinear lumped elements are included. The candidate terms are listed as follows

$$\frac{\partial u}{\partial t} = f \left(u, \frac{\partial u}{\partial z}, \frac{\partial^2 u}{\partial z^2}, \frac{\partial^3 u}{\partial z^3}, u \frac{\partial u}{\partial z}, u^2 \frac{\partial u}{\partial z}, u^3 \frac{\partial u}{\partial z}, u \frac{\partial^2 u}{\partial z^2}, u^2 \frac{\partial^2 u}{\partial z^2}, \dots, u^3 \frac{\partial^3 u}{\partial z^3} \right) \tag{23}$$

Then, based on the collected data, we calculate the matrix \mathbf{U}_t and Θ by the central difference formula for the linear equation $\mathbf{U}_t = \Theta \beta$. Finally, through the ridge regression, two active terms with non-zero weights β , namely $\frac{\partial^3 u}{\partial z^3}$ and $u \frac{\partial u}{\partial z}$, are identified from the library. The identified governing partial differential equation is shown in Eq. (25). By comparing with the actual governing equation in Eq. (24), it can be seen that our proposed method discovers the governing equation in the nonlinear lumped transmission line very well.

$$\frac{\partial u}{\partial t} + 6u \frac{\partial u}{\partial z} + \frac{\partial^3 u}{\partial z^3} = 0 \text{ (Actual form)} \tag{24}$$

$$\frac{\partial u}{\partial t} + 6.07u \frac{\partial u}{\partial z} + 1.03 \frac{\partial^3 u}{\partial z^3} = 0 \text{ (Identified form)} \tag{25}$$

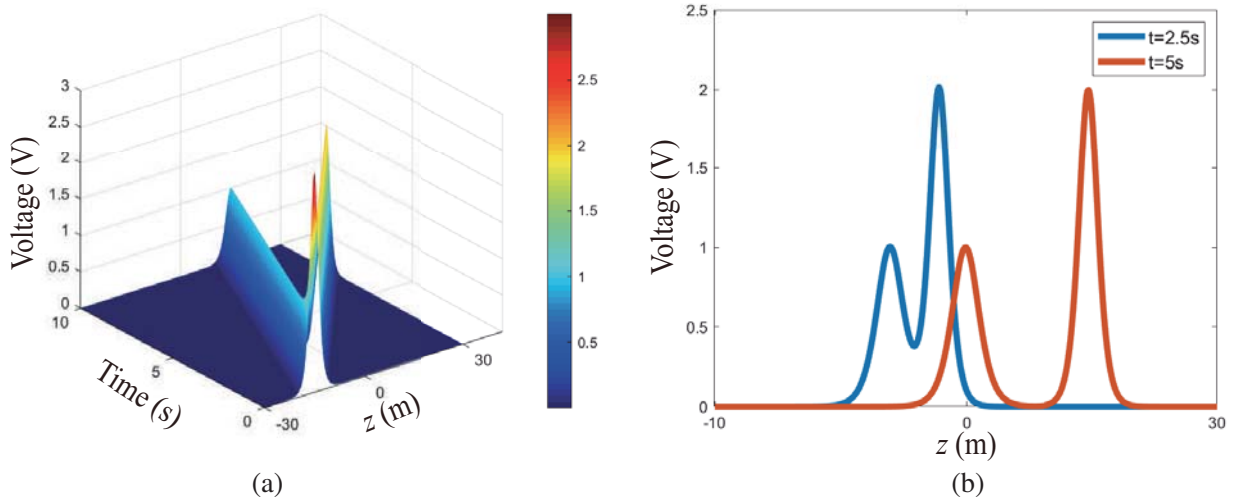


Figure 7. (a) The spatial-temporal voltage distribution. (b) The voltage distribution with time of 2.5 s and 5 s.

To simulate the real measurement environment, we add the white Gaussian noise into the input data with the signal to noise ratio (SNR) of 40 dB. The identified equation is also shown in Eq. (26). It can be seen that while the error of the inversion parameters increases due to the noise, the governing equations can also be identified to reveal the dynamics and thereby gain physical insights of the transmission line systems.

$$\frac{\partial u}{\partial t} + 6.16u \frac{\partial u}{\partial z} + 1.13 \frac{\partial^3 u}{\partial z^3} = 0 \text{ (Result with noise)} \quad (26)$$

The relative computer capacity of all the simulation is Intel (R) Core (TM) CPU (2.9 GHz, 16.0 GB). The simulation times for Fig. 3, Fig. 5, and Fig. 7 are 8.4090 s, 41.5210 s, and 1.8910 s, respectively. Additionally, it is worth noting that, for the lossy uniform transmission line, the voltage and current are the complex-valued solution. Several advanced methods like the physics informed neural networks [24, 46] have been developed to identify governing partial differential equations (PDE) for complex-valued data. For the sparse identification method, the complex-valued loss function could be adopted in the regression framework to determine the active spatial differential terms in the future.

4. CONCLUSION AND DISCUSSION

In summary, we demonstrated a novel data-driven approach to discover the governing partial differential equations in linear and nonlinear transmission line systems. The proposed method constructs a linear equation merely based on the spatial-temporal data to represent the general form of dynamics of the current and voltage signal. Ridge regression was established to derive the active spatial differential terms and identify the governing equations. We demonstrated the validity of the proposed approach in analyzing uniform, nonuniform, and nonlinear transmission lines. The governing partial differential equations for all the cases have been extracted. The obtained line parameters are also consistent with the theoretical results. Therefore, our work provides a practical data-driven tool for the modeling of transmission line systems, especially for the nonlinear lumped system.

ACKNOWLEDGMENT

This work was supported in part by the Research Grants Council of Hong Kong under Grant GRF 17209918, Grant GRF 17207114, and Grant GRF 17210815, and in part by the Asian Office of Aerospace Research and Development under Grant FA2386-17-1-0010.

APPENDIX A. IMPLEMENTATION OF FDTD

First, we discretize the current and voltage in the time domain based on the interval of Δt , respectively. Combining the spatial grids as shown in Fig. 3, the time and spatial discretization scheme is obtained and plotted in Fig. A1, where j and k refer to the indices of the spatial grids and time grids, respectively.

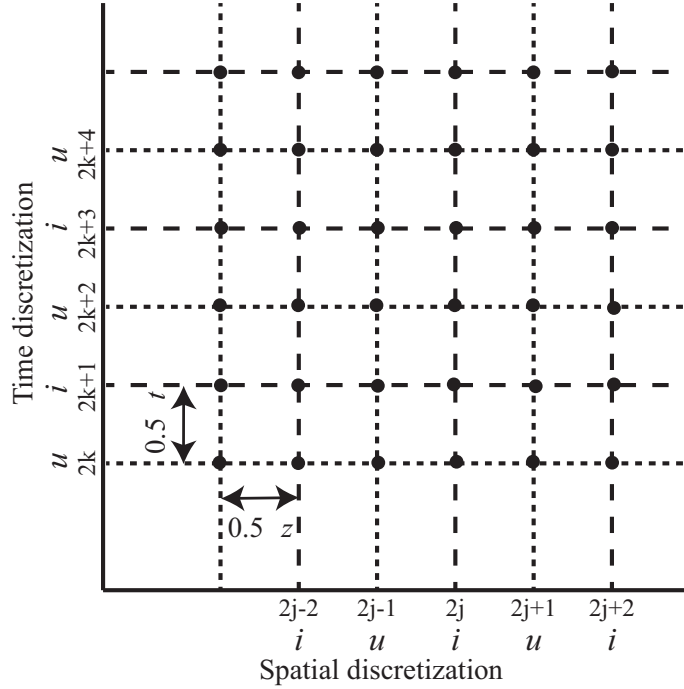


Figure A1. Time and spatial discretization of the voltages and currents.

Then, the central difference is utilized to take the time and spatial derivatives, which can be expressed as

$$\frac{\partial u}{\partial z} = \frac{u_{2j+1}^{2(k+1)} - u_{2j-1}^{2(k+1)}}{\Delta z} \tag{A1}$$

$$\frac{\partial i}{\partial z} = \frac{i_{2(j+1)}^{2k+1} - i_{2j}^{2k+1}}{\Delta z}$$

$$\frac{\partial u}{\partial t} = \frac{u_{2j+1}^{2(k+1)} - u_{2j+1}^{2k}}{\Delta t} \tag{A2}$$

$$\frac{\partial i}{\partial t} = \frac{i_{2j}^{2(k+1)+1} - i_{2j}^{2k+1}}{\Delta t}$$

Substituting Eqs. (A1) and (A2) into Eq. (17), one can obtain

$$u_{2j+1}^{2(k+1)} = \frac{\Delta t}{C} \left[\left(\frac{C}{\Delta t} - G \right) u_{2j+1}^{2k} + \frac{i_{2(j+1)}^{2k+1} - i_{2j}^{2k+1}}{\Delta z} \right] \tag{A3}$$

$$i_{2j}^{2(k+1)+1} = \frac{\Delta t}{L} \left[\left(\frac{L}{\Delta t} - R \right) i_{2j}^{2k+1} + \frac{u_{2j-1}^{2(k+1)} - u_{2j+1}^{2(k+1)}}{\Delta z} \right] \tag{A4}$$

Finally, we derive the updating equation based on the Kirchoff's circuit laws for the grids on both ends. The voltage-current relationship at the first end is given as

$$u_1^{2(k+1)} = v^{2k} - R_1 i_2^{2k+1} \tag{A5}$$

And the voltage-current relationship at the second end is expressed as

$$u_{2M+1}^{2(k+1)} = \frac{\Delta t}{C\Delta z} \left[\left(\frac{C\Delta z}{\Delta t} - G\Delta z - \frac{1}{R_2} \right) u_{2M+1}^{2k} + i_{2M}^{2k+1} \right] \quad (\text{A6})$$

The above updating equations are implemented via MATLAB in our simulations.

REFERENCES

1. Stinehelfer, H. E., "An accurate calculation of uniform microstrip transmission lines," *IEEE Trans. Microw. Theory Tech.*, Vol. 16, No. 7, 439–444, 1968.
2. Edward, G. C., "Theory and design of transmission line all-pass equalizers," *IEEE Trans. Microw. Theory Tech.*, Vol. 17, No. 1, 28–38, 1969.
3. Kimionis, J., A. Collado, M. M. Tentzeris, and A. Georgiadis, "Octave and decade printed uwb rectifiers based on nonuniform transmission lines for energy harvesting," *IEEE Trans. Microw. Theory Tech.*, Vol. 65, No. 11, 4326–4334, 2017.
4. Zhao, Y., S. Hemour, T. Liu, and K. Wu, "Nonuniformly distributed electronic impedance synthesizer," *IEEE Trans. Microw. Theory Tech.*, Vol. 66, No. 11, 4883–4897, 2018.
5. Ramirez, A. I., A. Semlyen, and R. Iravani, "Modeling nonuniform transmission lines for time domain simulation of electromagnetic transients," *IEEE Trans. Power Deliv.*, Vol. 18, No. 3, 968–974, 2003.
6. Lu, K., "An efficient method for analysis of arbitrary nonuniform transmission lines," *IEEE Trans. Microw. Theory Tech.*, Vol. 45, No. 1, 9–14, 1997.
7. Nikoo, M. S. and S. M.-A. Hashemi, "New soliton solution of a varactor-loaded nonlinear transmission line," *IEEE Trans. Microw. Theory Tech.*, Vol. 65, No. 11, 4084–4092, 2017.
8. Schleder, G. R., A. C. M. Padilha, C. M. Acosta, M. Costa, and A. Fazzio, "From DFT to machine learning: Recent approaches to materials science — A review," *J. Phys. Materials*, Vol. 2, No. 3, 032001, 2019.
9. Iten, R., T. Metger, H. Wilming, L. Del Rio, and R. Renner, "Discovering physical concepts with neural networks," *Phys. Rev. Lett.*, Vol. 124, No. 1, 010508, 2020.
10. Sugihara, G., R. May, H. Ye, C.-H. Hsieh, E. Deyle, M. Fogarty, and S. Munch, "Detecting causality in complex ecosystems," *Science*, Vol. 338, No. 6106, 496–500, 2012.
11. Ye, H., R. J. Beamish, S. M. Glaser, S. C. H. Grant, C.-H. Hsieh, L. J. Richards, J. T. Schnute, and G. Sugihara, "Equation-free mechanistic ecosystem forecasting using empirical dynamic modeling," *Proc. Natl. Acad. Sci. U. S. A.*, Vol. 112, No. 13, E1569–E1576, 2015.
12. Kevrekidis, I. G., C. William Gear, J. M. Hyman, P. G. Kevrekidid, O. Runborg, C. Theodoropoulos, et al., "Equation-free, coarse-grained multiscale computation: Enabling microscopic simulators to perform system-level analysis," *Commun. Math. Sci.*, Vol. 1, No. 4, 715–762, 2003.
13. Voss, H. U., P. Kolodner, M. Abel, and J. Kurths, "Amplitude equations from spatiotemporal binary-fluid convection data," *Phys. Rev. Lett.*, Vol. 83, No. 17, 3422, 1999.
14. Guo, L. and S. A. Billings, "Identification of partial differential equation models for continuous spatio-temporal dynamical systems," *IEEE Trans. Circuits Syst. II — Express Briefs*, Vol. 53, No. 8, 657–661, 2006.
15. Guo, L. Z., S. A. Billings, and D. Coca, "Identification of partial differential equation models for a class of multiscale spatio-temporal dynamical systems," *Int. J. Control*, Vol. 83, No. 1, 40–48, 2010.
16. Gonzalez-Garcia, R., R. Rico-Martinez, and I. G. Kevrekidis, "Identification of distributed parameter systems: A neural net based approach," *Comput. Chem. Eng.*, Vol. 22, S965–S968, 1998.
17. Giannakis, D. and A. J. Majda, "Nonlinear Laplacian spectral analysis for time series with intermittency and low-frequency variability," *Proc. Natl. Acad. Sci. U. S. A.*, Vol. 109, No. 7, 2222–2227, 2012.

18. Roberts, A. J., “Model emergent dynamics in complex systems,” *SIAM*, Vol. 20, 2014.
19. Majda, A. J., C. Franzke, and D. Crommelin, “Normal forms for reduced stochastic climate models,” *Proc. Natl. Acad. Sci. U. S. A.*, Vol. 106, No. 10, 3649–3653, 2009.
20. Daniels, B. C. and I. Nemenman, “Automated adaptive inference of phenomenological dynamical models,” *Nat. Commun.*, Vol. 6, No. 1, 1–8, 2015.
21. Bongard, J. and H. Lipson, “Automated reverse engineering of nonlinear dynamical systems,” *Proc. Natl. Acad. Sci. U. S. A.*, Vol. 104, No. 24, 9943–9948, 2007.
22. Schmidt, M. and H. Lipson, “Distilling free-form natural laws from experimental data,” *Science*, Vol. 324, No. 5923, 81–85, 2009.
23. Raissi, M. and G. E. Karniadakis, “Hidden physics models: Machine learning of nonlinear partial differential equations,” *J. Comput. Phys.*, Vol. 357, 125–141, 2018.
24. Raissi, M., P. Perdikaris, and G. E. Karniadakis, “Physics informed deep learning (part II, Data-driven discovery of nonlinear partial differential equations,” arxiv. arXiv preprint arXiv:1711.10561, 2017.
25. Long, Z., Y. Lu, and B. Dong, “PDE-Net 2.0: Learning pdes from data with a numericsymbolic hybrid deep network,” *J. Comput. Phys.*, Vol. 399, 108925, 2019.
26. Brunton, S. L., J. L. Proctor, and J. N. Kutz, “Discovering governing equations from data by sparse identification of nonlinear dynamical systems,” *Proc. Natl. Acad. Sci. U. S. A.*, Vol. 113, No. 15, 3932–3937, 2016.
27. Schaeffer, H., “Learning partial differential equations via data discovery and sparse optimization,” *Proc. R. Soc. A — Math. Phys. Eng. Sci.*, Vol. 473, No. 2197, 20160446, 2017.
28. Rudy, S. H., S. L. Brunton, J. L. Proctor, and J. N. Kutz, “Data-driven discovery of partial differential equations,” *Sci. Adv.*, Vol. 3, No. 4, e1602614, 2017.
29. Champion, K., B. Lusch, J. N. Kutz, and S. L. Brunton, “Data-driven discovery of coordinates and governing equations,” *Proc. Natl. Acad. Sci. U. S. A.*, Vol. 116, No. 45, 22445–22451, 2019.
30. Mangan, N. M., S. L. Brunton, J. L. Proctor, and J. N. Kutz, “Inferring biological networks by sparse identification of nonlinear dynamics,” *IEEE Trans. Mol. Biol. Multi-Scale Commun.*, Vol. 2, No. 1, 52–63, 2016.
31. Himanen, L., A. Geurts, A. S. Foster, and P. Rinke, “Data-driven materials science: Status, challenges, and perspectives,” *Adv. Sci.*, Vol. 6, No. 21, 1900808, 2019.
32. Murphy, K. P., *Machine Learning: A Probabilistic Perspective*, MIT Press, 2012.
33. Hoerl, A. E. and R. W. Kennard, “Ridge regression: Biased estimation for nonorthogonal problems,” *Technometrics*, Vol. 12, No. 1, 55–67, 1970.
34. LeVeque, R. J., “Finite difference methods for ordinary and partial differential equations: Steady-state and time-dependent problems,” *SIAM*, Vol. 98, 2007.
35. Nathan Kutz, J., *Data-driven Modeling & Scientific Computation: Methods for Complex Systems & Big Data*, Oxford University Press, 2013.
36. Elsherbeni, A. Z., V. Demir, et al., *The Finite-Difference Time-Domain Method for Electromagnetics with MATLAB Simulations*, SciTech Pub., 2009.
37. Knowles, I. and R. J. Renka, “Methods for numerical differentiation of noisy data,” *Electron. J. Differ. Equ.*, Vol. 21, 235–246, 2014.
38. Bruno, O. and D. Hoch, “Numerical differentiation of approximated functions with limited order-of-accuracy deterioration,” *SIAM J. Numer. Anal.*, Vol. 50, No. 3, 1581–1603, 2012.
39. Nevels, R. and J. Miller, “A simple equation for analysis of nonuniform transmission lines,” *IEEE Trans. Microw. Theory Tech.*, Vol. 49, No. 4, 721–724, 2001.
40. Watanabe, K., T. Sekine, and Y. Takahashi, “A FDTD method for nonuniform transmission line analysis using Yee’s-lattice and wavelet expansion,” *2009 IEEE MTT-S International Microwave Workshop Series on Signal Integrity and High-Speed Interconnects*, 83–86, 2009.
41. Sebastiano, G., S., P. Pantano, and P. Tucci, “An electrical model for the Korteweg-de Vries equation,” *Am. J. Phys.*, Vol. 52, No. 3, 238–243, 1984.

42. Ludu, A., *Nonlinear Waves and Solitons on Contours and Closed Surfaces*, Springer Science & Business Media, 2012.
43. Darling, J. D. C. and P. W. Smith, "High-power pulsed RF extraction from nonlinear lumped element transmission lines," *IEEE Trans. Plasma Sci.*, Vol. 36, No. 5, 2598–2603, 2008.
44. Kuek, N. S., A. C. Liew, E. Schamiloglu, and J. O. Rossi, "Circuit modeling of nonlinear lumped element transmission lines including hybrid lines," *IEEE Trans. Plasma Sci.*, Vol. 40, No. 10, 2523–2534, 2012.
45. Ricketts, D. S., X. Li, M. DePetro, and D. Ham, "A self-sustained electrical soliton oscillator," *IEEE MTT-S International Microwave Symposium Digest*, 4, IEEE, 2005.
46. Raissi, M., A. Yazdani, and G. E. Karniadakis, "Hidden fluid mechanics: Learning velocity and pressure fields from flow visualizations," *Science*, Vol. 367, No. 6481, 1026–1030, 2020.